

Ionization in fast atom-atom collisions: The influence and scaling behavior of electron-electron and electron-nucleus interactions

J. M. Sanders

Department of Physics, University of South Alabama, Mobile, Alabama 36688, USA

R. D. DuBois

Department of Physics, University of Missouri–Rolla, Rolla, Missouri 65401, USA

S. T. Manson

Department of Physics and Astronomy, Georgia State University, Atlanta, Georgia 30303, USA

S. Datz,^{*} E. F. Deveney,[†] H. F. Krause, J. L. Shinpaugh,[‡] and C. R. Vane
Physics Division, Oak Ridge National Laboratory, Oak Ridge, Tennessee 37831, USA

(Received 11 September 2007; published 28 December 2007)

We report cross sections for ionization of He coincident with electron loss from He, Li, C, O, and Ne projectiles. For He, Li, C, and O projectiles, the cross sections were measured directly, while the Ne cross sections were obtained by transforming results for He projectiles colliding with Ne. We find that, at energies of about 100–500 keV/u, neutral projectiles can ionize a He target almost as effectively as a charged projectile. The contribution to ionization due to electron-electron interactions is found to scale with the number of available projectile electrons. Comparing ionization by the bound electrons on projectiles to ionization by free electrons, we find that the cross sections for ionization by bound electrons are systematically smaller than those for free electrons.

DOI: [10.1103/PhysRevA.76.062710](https://doi.org/10.1103/PhysRevA.76.062710)

PACS number(s): 34.50.Fa

I. INTRODUCTION

In contrast to the vast number of experiments that have explored ion-atom collisions in great detail, relatively little experimental information is available about energetic atom-atom interactions. This lack of information is unfortunate in light of the fact that all energetic ions passing through gaseous or condensed-phase media slow down and capture electrons. If the medium is thick enough, at some point their charge will be totally neutralized. In subsequent interactions, these neutral projectiles can ionize the medium or be ionized themselves. Thus, information about fast atom-atom collisions as a function of impact energy has a practical importance relating to energy deposition and track structure models.

Energetic atom-atom collisions are also of fundamental interest, since they represent a unique subset of dressed ion-atom collisions. Here “dressed” is used to indicate that the incoming particle possesses bound electrons prior to the collision. Interactions between two neutral particles provide a unique proving ground to study inelastic processes where no long-range Coulomb forces are present along the incoming trajectory. At first glance one might expect that the interaction cross sections in atom-atom collisions would be much smaller than those induced by their singly charged ion coun-

terparts, e.g., target ionization induced by H versus H⁺ impact. However, experimental studies [1–3] have shown that targets are ionized by neutral atoms nearly as efficiently as by singly charged ions.

Neutral projectiles are effective ionizers, because there are two ionization mechanisms which operate for dressed particle impact (meaning either neutral atoms or partially stripped ions). The first mechanism, sometimes referred to as the electron-nuclear interaction, as a singly inelastic process, or as the screening contribution, results from Coulomb interactions between the partially screened nuclear charge of one collision partner and electrons bound to the other partner. In this paper we shall use the term electron-nuclear (*e-n*) when referring to these processes. The *e-n* cross sections scale as the square of an effective projectile charge Z_{eff} , which is generally determined by comparing cross sections measured for partially stripped ion impact with those measured for fully stripped ion impact and assuming that the cross sections scale as Z_{eff}^2 . By this method, it is typically found for low-charge-state ions that $Z_{\text{eff}} \approx q$, the net charge.

The second ionization mechanism involves direct interactions between target and projectile electrons. In this mechanism, both electrons are excited or ionized. As this present paper is concerned with liberating electrons to the continuum, the term ionization will generally be used, but the following descriptions and discussions also apply to exciting electrons to discrete states. This second mechanism has been referred to as the electron-electron interaction, as a doubly inelastic process, or as the antiscreening term. Here we shall use the term electron-electron interaction, designated as *e-e*. As pointed out previously [4], *e-e* processes are expected to scale with the number of loosely bound projectile electrons, N .

^{*}Deceased.

[†]Present address: Department of Physics, Bridgewater State College, Bridgewater, MA 02325, USA.

[‡]Present address: Department of Physics, East Carolina University, Greenville, NC 27858, USA.

Some years ago, DuBois and Manson [4] investigated these e - e scaling predictions. Using experimental data and theoretical arguments for H and He atom impact ionization of helium, they concluded that e - e processes dominated the total target ionization cross sections for fast atom impact. In the present paper, we reconsider this question in more detail and consider a more extensive set of neutral projectiles. We will present data for helium atom impact data for impact energies between 12.5 and 500 keV/u and data for atomic lithium, carbon, and oxygen impact for selected energies between 100 and 500 keV/u. In addition, data for atomic helium impact on neon between 25 and 500 keV/u are presented. In all cases, coincidences between projectile and target ions and between neutral projectiles and target ions were measured. When combined with total electron loss cross sections for projectile ionization which were measured or taken from the literature, we are able to investigate single- and multiple-electron removal processes from either the target or from the projectile, or from both, over a fairly broad range of impact energies and projectile Z . Also, by exchanging the roles of target and projectile, the He-Ne data allow us to investigate the relative importance of e - e versus e - n processes and their scaling behavior over a broader range of projectile Z than previously possible.

II. THEORETICAL EXPECTATIONS AND SCALING BEHAVIOR FOR e - n AND e - e PROCESSES

A theoretical description of inelastic atomic processes, using the Born approximation, was presented many years ago by Bates and Griffing [5] and Bell *et al.* [6,7]. Later, similar Born formulations were employed to calculate differential electron emission cross sections for partially stripped ion impact [8–10]. To outline the various processes and their scaling behavior, we shall use the nomenclature of Ref. [10] and restrict ourselves to ionization processes; although, as stated in the Introduction, many of the same arguments and conclusions also apply for excitation processes.

In the Born approximation, the doubly differential cross sections for target ionization by a dressed projectile with net charge $q=Z-N$, where Z is the nuclear charge and N is the number of bound electrons, are given by the sum of two contributions:

$$d^2\sigma_{e-n}(\epsilon) = \int_{K_{\min}}^{K_{\max}} A(\epsilon, K)[Z - NF(K)]^2 dK \quad (1)$$

and

$$d^2\sigma_{e-e}(\epsilon) = \int_{K'_{\min}}^{K'_{\max}} A(\epsilon, K)[N - N|F(K)|^2] dK. \quad (2)$$

Here $d^2\sigma(\epsilon)$ is the differential cross section for liberating an electron of energy ϵ , $A(\epsilon, K)$ contains all information about the target atom from which the electron is liberated, and $F(K)$ is the single-electron form factor as a function of momentum transfer K for the initial state of the collision partner (projectile), i.e., $F(K) = \langle i | e^{iK \cdot r} | i \rangle$. By definition, $0 < |F| < 1$ for $0 < K < \infty$, which corresponds to large- and small-impact-

parameter collisions, respectively. Note that the integrations are from some minimum momentum transfer to some maximum value and that the two limits are different in the two equations. The reader is referred to Ref. [10] for additional details.

Equation (1) describes interactions where the bound projectile electrons play a passive role in the collision, i.e., they simply serve to partially screen the projectile nuclear charge. These are the e - n interactions discussed in the Introduction. In these interactions the target is ionized, while the projectile remains in the ground state. For e - n processes, the cross section scales as the square of an effective projectile charge Z_{eff} , which is the bracketed term in Eq. (1). Also note that Z_{eff} depends on the momentum transfer and, hence, on the impact parameter, but for total (integral) cross sections the standard experimental definition is to use an average value determined by comparing cross sections measured for partially and fully stripped ion impact. As a result of such comparisons, it is found that $Z_{\text{eff}} \approx q$, and, since $q \leq Z$, the ionization cross sections resulting from e - n processes are smaller for dressed ion impact than for fully stripped ion impact.

Equation (2) describes direct interactions between projectile and target electrons. These e - e processes result in both the target and the projectile electrons being excited or ionized, which requires the minimum momentum transfer to be larger than for e - n processes. Also, because the “collision” is now between two electrons rather than between a heavy nucleus and an electron, the maximum momentum transfer is smaller for e - e processes than for e - n processes. In spite of these narrower limits, e - e processes imply a larger ionization cross section for dressed ion impact than for fully stripped ion impact, since they are present for one but not the other. Finally, note that Eq. (2) implies that e - e processes should scale linearly with the number of electrons bound to the incoming projectile, N .

Before going into more detail on the scaling behaviors, note that the above formulas can also be used to determine ionization of the projectile. In this case, the roles of the projectile and target quantities in the above discussion are interchanged, the projectile ionization cross sections are calculated, and a transformation is made to the laboratory frame of reference.

We now turn our attention to what Eqs. (1) and (2) predict about the relative importance of e - e and e - n processes and what scaling dependences are expected for different collision systems. As was pointed out previously, the major differences between Eq. (1) and Eq. (2) are the bracketed terms [10]. In Table I are values of the bracketed terms for various momentum transfer K . Recall that K varies from 0 to ∞ as the impact parameter varies from ∞ to 0, and over this range $F(K)$ varies from 1 to 0. Thus, using the extreme values for the electron form factor F , we obtain estimates of the relative importance of e - e and e - n processes for large- and small-impact-parameter collisions; we also obtain how the e - e and e - n contributions should scale as a function of the projectile Z and the number of bound electrons, N . This is done for all types of dressed particles, namely, for partially stripped ion and for neutral atom impact. For dressed ion impact, the maximum relative importance of the e - e process is also ob-

TABLE I. Scaling relations for $e-e$ and $e-n$ contributions to the ionization cross section for different momentum transfer regimes. The $K \rightarrow 0$ limit implies that $F=1-\epsilon$ for $\epsilon \rightarrow 0$. The ratio $(e-e)/(e-n)$ is maximized for ion projectiles when $F=N/Z$. Finally, the $K \rightarrow \infty$ limit implies $F=\epsilon$ with $\epsilon \rightarrow 0$.

	Ion impact			Neutral impact ($Z=N$)		
	$e-e$	$e-n$	$(e-e)/(e-n)$	$e-e$	$e-n$	$(e-e)/(e-n)$
$K \rightarrow 0$	$2\epsilon N$	$(Z-N)^2$	$\epsilon N / (Z-N)^2$	$2\epsilon N$	$\epsilon^2 N^2$	$1 / \epsilon N \rightarrow \infty$
	$N[(Z^2-N^2)]/Z$	$(Z^2-N^2)^2/Z^2$	N/Z^2-N^2			
$K \rightarrow \infty$	N	Z^2	$\epsilon N / Z^2$	N	N^2	$1/N$

tained since, unlike the situation for neutral particle impact, it does not occur when $F=1$.

As shown in Table I, for neutral particle impact the relative importance of $e-e$ interactions is maximum and in fact dominates for large impact parameters ($K \rightarrow 0$). This implies that $e-e$ interactions should dominate the total ionization cross section, since total cross sections are largely determined by large-impact-parameter collisions. In contrast, for partially stripped ion impact, the relative importance of $e-e$ processes is maximized at some intermediate impact parameter (momentum transfer) and the ratio $(e-e)/(e-n)$ is always less than 0.5, which is the limiting value for singly charged very heavy ions (i.e., $N=Z-1$ and $Z \rightarrow \infty$). As for scaling expectations, total cross sections for target ionization by fast, neutral atom impact should scale linearly with the number of bound electrons for the $e-e$ process whereas the $e-n$ process should show a quadratic dependence with N .

Since the $e-e$ process involves direct interactions between projectile and target electrons, it is a special type of electron impact ionization process, the differences being that in $e-e$ ionization processes, the minimum energy transfer is the sum of the projectile and target electron binding energies, whereas for electron impact it is only the target binding energy. Also, for the $e-e$ process, the projectile electrons do not impact with a single fixed velocity but rather with a velocity distribution centered on the projectile velocity. However, for impact energies far above threshold, $e-e$ cross sections should be comparable to electron impact cross sections multiplied by N .

In the next section, we describe how cross sections appropriate for testing these predictions were obtained using projectile-target ion coincidence techniques. It is important to emphasize that the $e-e$ process is a first-order process which results in ionization or excitation of both collision partners whereas the $e-n$ process ionizes (or excites) only one of the partners. Thus, information about $e-e$ processes can be obtained by measuring events where both the projectile and the target are ionized. However, keep in mind that second-order processes, i.e., $(e_i-n_p)(e_p-n_i)$, where the target and projectile quantities are explicitly designated, also can ionize both collision partners. Since at higher energies the first-order ($e-e$) process will dominate [11], data of the type presented here are required at the highest impact energy possible. We would like to point out that an alternative method (recoil ion momentum spectroscopy) exists which can distinguish between these first- and second-order processes [12–15]. Also, keep in mind that the coincidence measurements are only sensitive to ionization processes and that, if

one of the partners is simply excited, not only will that flux be absent from the process of interest but it may be interpreted as being part of a different process. For example, in a H-He collision, if H is excited and He is ionized via an $e-e$ interaction, this signal will experimentally appear as a coincidence between a nonionized projectile and an ionized target, and it would falsely be included in the $e-n$ channel. Our method could not distinguish this problem although in principle recoil ion spectroscopy could. Typically, however, in the collisions studied here, these excitation-ionization processes are expected to make minor contributions relative to ionization-ionization processes, simply because the phase space is much smaller.

III. EXPERIMENTAL METHODS

A. Methods for He and Ne data

Data presented here were obtained at two different laboratories using entirely different experimental setups. The He-He and He-Ne data were measured at the Pacific Northwest Laboratories using methods previously described [1,16–18]. The only difference in the present work relates to the production of a neutral helium beam. This was done by using electron capture reactions to neutralize a portion of an energetic He⁺ beam extracted from a Van de Graaff accelerator. Strong electrostatic fields, approximately 1–2 kV/cm, immediately after the charge exchange cell and just before the target region were used to prevent any charged components of the beam from entering the interaction volume. An electrostatic charge state analyzer immediately following the target (approximately 4 cm downstream) was used to direct the desired postcollision projectile charge state on a movable channeltron detector, which counted the secondary electron emission from a metal plate. Data were collected first with no charge state analysis, so all charge states were counted together. Then the analyzer was adjusted to allow each of the possible charge components, i.e., -1 , 0 , $+1$, and $+2$, to be counted. For each case, the total number of extracted target ions was recorded. These data were normalized to each other using this information. To place them on an absolute scale, detection efficiencies for both the projectile and target detectors were taken from Refs. [16–18], and measurements using He⁺ impact were performed and normalized to absolute cross sections [18] to calibrate the target density and overall target ion extraction efficiency. Once these parameters were known, identical experimental conditions were used to measure the He impact cross sections. To establish relative un-

certainties, measurements were repeated at selected impact energies. As a result, it was found that reproducibility errors were typically better than $\pm 15\%$ except for the smallest cross sections measured, where reproducibility was $\pm 50\%$ to 100% due to low statistics and other factors. After including errors associated with detection efficiencies and normalization, the absolute data presented here are considered to be accurate to approximately $\pm 25\%$ to 30% .

These uncertainties do not account for any influence on the measured cross sections due to long-lived metastable components of the helium beam. From comparison of stripping cross sections which we measured using standard growth curve techniques with those reported by Pedersen *et al.* [19] for ground and excited state He impact and using the relative amounts of excited and ground state atoms they quoted for producing neutral beams using a technique similar to ours, it was concluded that our atomic helium beams contained a 25–30% metastable component. Thus, our reported cross sections are subject to systematic errors associated with metastable atom impact. We should mention that the present data were measured some years ago but publication was delayed precisely because of this concern over unknown systematic errors. However, there is virtually no experimental information in the literature on this simple and fundamentally important collision system. Thus, these data are presented with the caution that the user must keep in mind the possible influence of metastable helium impact on the quoted cross sections.

B. Methods for Li, C, and O data

The lithium, carbon, and oxygen atom impact data were obtained using the ORNL EN tandem Van de Graaff facility. Beams of singly charged Li, C, and O ions were extracted, momentum analyzed, and then neutralized in a gas cell. As the beam emerged from the neutralizing cell, it passed between the poles of a permanent magnet which served to remove any remaining ions from the beam. The beam then passed through a 3.2-cm-long target gas cell after which the projectiles were charge-state analyzed by an electrostatic field and counted using a position-sensitive detector consisting of a microchannel plate chevron and a resistive anode encoder.

An electric field extracted recoil ions from the target cell. The recoil ions then passed through a field-free drift region and were accelerated onto a microchannel plate detector. The signals from the recoil and projectile detectors started and stopped, respectively, a time-to-amplitude converter whose output generated a time-of-flight spectrum of the recoil ions. Coincidence spectra of the projectile position and the recoil time of flight allowed the identification of the final projectile and recoil charge states.

These coincidence data were placed on an absolute scale by first measuring total capture and loss cross sections for each neutral beam using the growth method. Fractions of the different charge states emerging from the target gas cell were determined for several target gas pressures and a generalized, least-squares, linear fit of the charge fraction ϕ_j as a function of pressure P yielded a slope proportional to the cross sec-

tion. The cross sections were obtained from the slope $d\phi_j/dP$, by

$$\sigma^{ij} = \frac{d\phi_j}{dP} \frac{kT}{l_{\text{eff}}}. \quad (3)$$

Here σ^{ij} is the cross section for production of a projectile of charge j from an incoming projectile of charge i , k is the Boltzmann constant, and l_{eff} is the effective length of the gas cell. The effective target gas cell length was found to be 5.7 cm, approximately 78% larger than the physical length, by normalizing our present total cross sections for single capture with those previously measured for 0.5 MeV/u C^{6+} on He [20–23], for single ionization by 0.5 MeV/u C^{6+} on He [24], for single ionization by 0.5 MeV/u Li^{3+} on He [25], for capture by 0.1 MeV/u C^{3+} on He [21], and for single loss, double loss, and capture by 0.1 MeV/u C on He [26].

Next, the coincidence spectra were accumulated for each beam at two different pressures within the single-collision regime in the gas cell. The yield of projectiles in each charge state coincident with the two recoil charge states was recorded and the cross section was calculated from

$$\sigma_n^{ij} = \frac{Y_n^{ij} kT}{PI\eta l_{\text{eff}}}. \quad (4)$$

Here σ_n^{ij} is the cross section for producing a He^{n+} ion while the projectile goes from charge state i to j , Y_n^{ij} is the yield of coincidence counts for the corresponding recoil and projectile charge states, and I is the total number of incident projectiles. The overall coincidence detection efficiency η was obtained by noting that the total single-charge transfer cross section must equal the sum of the pure capture and transfer ionization cross sections, i.e., $\sigma^{j,i-1} = \sigma_1^{j,i-1} + \sigma_2^{j,i-1}$. This last expression and Eq. (4) can be solved for η in terms of measured coincidence yields and the total charge transfer cross section:

$$\eta = \frac{Y_1^{i,i-1} - Y_2^{i,i-1} kT}{PI\sigma^{i,i-1} l_{\text{eff}}}. \quad (5)$$

By this method, efficiencies were calculated using a wide variety of beam energies and charge states. The average value of these separate measurements was used in Eq. (4) to determine individual absolute cross sections. Uncertainties associated with detector efficiency and normalization procedures are on the order of $\pm 15\%$. Each coincident cross section was repeated at different pressures in the single-collision regime, and the results were averaged. The uncertainty in the average provides a measure of the reproducibility error in the measurements which were typically of the order of $\pm 10\%$ except for the smaller cross sections, where the reproducibility error rose to $\pm 30\%$.

IV. RESULTS AND DISCUSSION

We will use the following notation for the ionization cross sections: σ_i^{0j} will represent the cross section where the final charge state of the target is i , and the projectile goes from charge 0 to charge j . The absolute cross sections obtained as

TABLE II. Cross sections for projectile and target ionization in He-He collisions in units of 10^{-16} cm². Uncertainties in the absolute cross sections are approximately $\pm 30\%$ except for the smallest cross sections measured, where they can be $\pm 50\%$ to 100% . HH indicates cross sections reported in Refs. [19] and [27] averaged for a 75% ground state and 25% excited state He atom beam (interpolated where necessary).

	<i>E/M</i> (keV/u)										
	12.5	18.75	25	37.5	50	75	100	175	250	375	500
σ_+	1.15	1.42	1.83	1.73	1.64	1.59	1.58	1.14	0.955	0.701	0.576
σ_-	2.48	2.72	3.36	3.40	3.21	3.09	2.75	2.03	1.76	1.35	1.06
σ_1^{00}	1.02	1.20	1.40	1.20	1.10	0.95	0.88	0.62	0.50	0.35	0.29
σ_2^{00}	0.012	0.015	0.037	0.048	0.055	0.060	0.055	0.029	0.020	0.0108	0.0075
σ_1^{0-1}	0.0041	0.0031	0.0068	0.0064	0.0057	0.0018	0.0011				
HH σ^{01}	1.30	1.22	1.15	1.28	1.27	1.18	1.09	0.823	0.794		
σ^{01}	1.33	1.31	1.50	1.60	1.50	1.40	1.05	0.79	0.74	0.61	0.46
σ_0^{01*}	1.22	1.13	1.16	1.18	1.10	0.925	0.522	0.373	0.355	0.302	0.205
σ_1^{01}	0.105	0.180	0.340	0.410	0.390	0.450	0.500	0.395	0.370	0.300	0.250
σ_2^{01}	0.0004	0.0013	0.0025	0.0065	0.0145	0.0250	0.0280	0.0225	0.0150	0.0081	0.0055
HH σ^{02}					0.038	0.052	0.058	0.049	0.034	0.019	0.012
σ^{02}			0.020	0.037		0.060					
σ_0^{02*}			0.0189	0.0319	0.029	0.0312	0.030	0.0278	0.0181	0.0065	0.0031
σ_1^{02}			0.0012	0.0051	0.0090	0.0175	0.0280	0.0195	0.0130	0.0111	0.0081
σ_2^{02}					0.00027	0.00135	0.00190	0.00173	0.00095	0.00090	0.00085

described in the previous section are given in Tables II–VI. Also included in these tables are total electron loss cross sections, σ^{0j} , which were taken from the literature or directly measured. By subtracting the sum of all the σ_i^{0j} from the total

σ^{0j} , cross sections for ionization of the projectile via the $e-n$ process were obtained. These are designated by σ_0^{0j*} , where the asterisk indicates that the value was obtained indirectly. Also included in the tables are total cross sections for target

TABLE III. Cross sections for projectile and target ionization in He-Ne collisions in units of 10^{-16} cm². Uncertainties in the absolute cross sections are approximately $\pm 30\%$ except for the smallest cross sections measured, where they can be $\pm 50\%$ to 100% . H indicates cross sections reported in Ref. [19] averaged for a 75% ground state and 25% excited state He atom beam (interpolated where necessary).

	<i>E/M</i> (keV/u)									
	25	37.5	50	75	100	175	250	375	500	
σ^+	2.98	3.45	3.79	3.72	4.06	3.09	2.76	2.08	1.66	
σ^-	5.18	5.64	6.30	6.35	7.11	5.89	5.35	4.01	3.49	
σ_1^{00}	1.56	1.44	1.44	1.15	1.05	0.755	0.672	0.499	0.400	
σ_2^{00}	0.252	0.311	0.296	0.279	0.255	0.136	0.098	0.058	0.037	
σ_3^{00}	0.0141	0.0249	0.0398	0.0490	0.0556	0.0191	0.0173	0.0066	0.0091	
σ_4^{00}			0.0138							
σ_1^{0-1}			0.0045	0.0025						
σ_2^{0-1}				0.00087						
H σ^{01}	1.90	2.10	2.35	2.35	2.60	2.23	2.05	1.65	1.53	
σ_0^{01*}	1.14	1.09	1.14	1.09	1.09	1.02	0.932	0.713	0.764	
σ_1^{01}	0.644	0.781	0.925	0.895	1.10	0.879	0.834	0.752	0.629	
σ_2^{01}	0.112	0.204	0.243	0.313	0.341	0.272	0.242	0.163	0.124	
σ_3^{01}	0.0033	0.0249	0.0440	0.0548	0.0706	0.0566	0.0416	0.0224	0.0125	
σ_4^{01}					0.0073	0.0065		0.0024	0.0024	
σ_1^{02}		0.0335	0.0572	0.0961	0.144	0.163	0.187	0.130	0.0924	
σ_2^{02}		0.0074	0.0173	0.0349	0.0641	0.0796	0.0781	0.0589	0.0468	
σ_3^{02}		0.0012	0.0015	0.0054	0.0116	0.0186	0.0198	0.0100	0.0120	
σ_4^{02}					0.0008	0.0035	0.0030	0.0024	0.0020	

TABLE IV. Cross sections for projectile and target ionization in Li-He collisions in units of 10^{-16} cm². Uncertainties in the absolute cross sections are approximately $\pm 30\%$ except for the smallest cross sections measured, where they can be $\pm 50\%$ to 100% .

	E/M (keV/u)		
	125	200	500
σ_1^{00}	0.87	0.78	0.59
σ_2^{00}	0.049	0.037	0.015
σ^{01}	0.92	0.86	0.41
σ_0^{01*}	0.43	0.36	0.069
σ_1^{01}	0.46	0.47	0.33
σ_2^{01}	0.033	0.029	0.011
σ^{02}	0.028	0.035	0.015
σ_0^{02*}	0.0061	0.0086	0.0005
σ_1^{02}	0.019	0.023	0.013
σ_2^{02}	0.0028	0.0034	0.0015

ionization, σ^+ , and for free electron production, σ^- , for the collision.

In the discussions that follow, we will focus on collisions of neutral projectiles with He targets; therefore, in order to use the He projectile on Ne target data, we will reverse the roles of the projectile and target. This reversal can be effected by a simple relabeling of the cross sections in Table III. The cross section σ_i^{0j} with a He target (He final charge state i and Ne final charge state j) will be found in Table III as σ_j^{0i} with a Ne target. In the remainder of this paper, it will be assumed that He is the target.

TABLE V. Cross sections for projectile and target ionization in C-He collisions in units of 10^{-16} cm². Uncertainties in the absolute cross sections are approximately $\pm 30\%$ except for the smallest cross sections measured, where they can be $\pm 50\%$ to 100% .

	E/M (keV/u)		
	100	300	500
σ_1^{00}	0.92	0.87	0.62
σ_2^{00}	0.092	0.090	0.055
σ^{0-1}	0.060	0.047	
σ_1^{0-1}	0.048	0.058	
σ_2^{0-1}	0.0058	0.00095	
σ^{01}	1.8	0.90	0.54
σ_0^{01*}	0.66	0.23	0.16
σ_1^{01}	0.99	0.59	0.34
σ_2^{01}	0.15	0.077	0.035
σ^{02}	0.33	0.13	0.058
σ_0^{02*}	0.048	0.027	0.0066
σ_1^{02}	0.23	0.083	0.043
σ_2^{02}	0.052	0.020	0.0084
σ^{03}	0.012	0.018	0.0086
σ_0^{03*}		0.0089	0.0026
σ_1^{03}	0.011	0.0069	0.0048
σ_2^{03}	0.0023	0.0022	0.0012

TABLE VI. Cross sections for projectile and target ionization in O-He collisions in units of 10^{-16} cm². Uncertainties in the absolute cross sections are approximately $\pm 30\%$ except for the smallest cross sections measured, where they can be $\pm 50\%$ to 100% .

	E/M (keV/u)
	100
σ_1^{00}	0.71
σ_2^{00}	0.086
σ^{0-1}	0.062
σ_1^{0-1}	0.049
σ_2^{0-1}	0.010
σ^{01}	1.3
σ_0^{01*}	0.46
σ_1^{01}	0.69
σ_2^{01}	0.15
σ^{02}	0.33
σ_0^{02*}	0.058
σ_1^{02}	0.21
σ_2^{02}	0.062
σ^{03}	0.039
σ_1^{03}	0.031
σ_2^{03}	0.011

With regard to the He-He collisions reported in Table II, our measured total loss cross sections are in quite good agreement with measurements by Pedersen *et al.* [19], if we assume that our beam had a 25% metastable component. How this influences the individual cross sections is impossible to say, but some clues can be obtained by comparing target and projectile ionization cross sections in this symmetric collision. For example, single and double ionization of the target can be compared to single and double loss from the projectile, if one keeps in mind that the target always is initially in the ground state whereas the projectile is sometimes in a metastable state. Doing such a comparison indicates that the perturbing effects to the present data by metastable projectiles are quite important below 200 keV/u, but are relatively unimportant at higher energies.

As discussed in Sec. II, the $e-n$ process results in the ionization of only one collision partner, so σ_1^{00} is the cross section for the $e-n$ process. The $e-e$ process results in the ionization of both collision partners, so σ_1^{01} is the cross section for the $e-e$ process [again, the $(e_r-n_p)(e_p-n_t)$ process could also lead to ionization of both partners, but it is a second-order process and is dominated by the first-order $e-e$ process at the high energies we consider here]. Therefore, to demonstrate the relative importance of $e-e$ versus $e-n$ processes for removing a single electron from the target, in Fig. 1 we plot the ratio $\sigma_1^{01}/\sigma_1^{00}$ as a function of impact energy for various collision systems. Also shown in the figure are the scaled binding energies of the projectile electrons.

Several things are immediately obvious from Fig. 1. First, for all neutral projectile velocities greater than the velocities of the bound projectile electrons, the relative importance of $e-e$ compared to $e-n$ ionization mechanisms tends to saturate

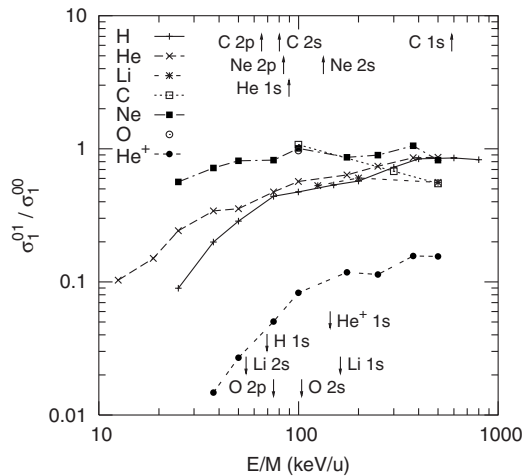


FIG. 1. Ratio $\sigma_1^{01}/\sigma_1^{00}$ for H, He, Li, C, O, and Ne colliding with He as a function of projectile energy. The ratio of cross sections qualitatively is the ratio of the importance of $e-e$ versus $e-n$ processes. Also shown by arrows in the figure are the thresholds for the various $e-e$ processes. For comparison, the ratio $\sigma_1^{12}/\sigma_1^{11}$ for He^+ colliding with He and its respective thresholds are also shown. The H and He^+ data are from Refs. [1] and [18], respectively.

at a value of 60–100 %. This saturation typically is reached for impact energies roughly four times that of the scaled threshold energy, i.e., $(M/m)[(E_{\text{bind}})_{\text{proj}} + (E_{\text{bind}})_{\text{targ}}]$. These threshold energies are shown in the figure. Here M and m are the projectile and electron masses, respectively, and E_{bind} are the binding energies for the target and projectile electrons [28]. Note that, for the heavier projectiles, the K -shell electrons are too tightly bound to be liberated in the present impact energy range and therefore do not participate in $e-e$ ionization processes. Second, note that the relative importance of $e-e$ versus $e-n$ processes is much smaller for singly charged ion impact. This qualitative feature is in accordance with the simple predictions given in Table I, although quantitatively the predicted ratios are much larger than those observed.

The second thing to note in this figure is that the ratios do not sharply drop in magnitude for impact energies below the thresholds shown. This is in part due to the momentum distribution of the projectile electrons and in part to the second-order $e-n$ mechanism which contributes to simultaneous ionization of both collision partners.

In Fig. 2 we test our simple scaling predictions presented above by plotting cross sections for target and projectile ionization via $e-n$ processes, e.g., $e-n_{\text{targ}}$ for projectile ionization by the partially screened target nucleus and $e-n_{\text{proj}}$ for target ionization by the partially screened projectile nucleus, and for $e-e$ processes, all data for 0.5 MeV/u collision energies, the highest energy our data allow. Also note that extrapolation of ground and metastable state cross sections given in Ref. [19] implies a minimal influence due to metastable contamination of our He beam. The $e-n$ cross sections are plotted versus the projectile Z while the $e-e$ processes are plotted versus the number of projectile electrons available to participate in the collision. From Fig. 1 we see that for 0.5 MeV/u

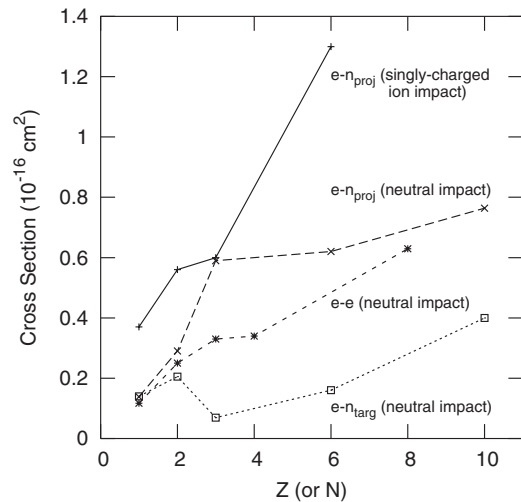


FIG. 2. Scaling of $e-e$, $e-n_{\text{proj}}$, and $e-n_{\text{targ}}$ as functions of N and Z_{eff} at 500 keV/u. Data for H are interpolated from data of Ref. [1]. Data for H^+ are from Ref. [25], for He^+ from Ref. [18], and for Li^+ and C^+ from the present experiment.

impact energies this means that $N=1, 2, 3, 4, 6$, and 8 for neutral H, He, Li, C, O, and Ne impact, respectively.

According to our scaling arguments, we expect the $e-e$ cross sections to increase linearly with N . Figure 2 shows that qualitatively this is correct, but quantitatively the increase is slightly slower. This difference may be significant, but we note that within experimental uncertainties a linear increase with N is observed.

Looking now at the $e-n$ cross sections we expect the $e-n_{\text{proj}}$ cross sections, i.e., ionization of helium by neutral atoms and singly charged ions, to scale as Z_{eff}^2 , where Z_{eff} is the partially screened projectile nuclear charge. Using the proton impact cross section as a standard, we found that Z_{eff} is 1.3 for He^+ and Li^+ impact, is approximately 2 for C^+ impact, and systematically increases from approximately 0.7 to 1.3 for H, He, and Li atom impact, after which it remains roughly constant up to Ne atom impact. More difficult to understand are the cross sections for ionization of various neutral projectiles by helium atoms, i.e., the $e-n_{\text{targ}}$ cross sections. Proton impact ionization cross sections for various atomic and molecular targets have been found to scale according to the number of loosely bound outer-shell target electrons [29–33]. This scaling is moderated to some degree by the binding energies of the electrons, i.e., more loosely bound electrons ionize much more easily than those with higher ionization potentials. Therefore, compared to the ionization cross sections of an H projectile, we would expect a slightly larger cross section for He, and much larger cross sections for Li, C, and Ne. These features generally are not seen.

Finally, in Fig. 3 we compare absolute cross sections for single ionization of helium by bound and free electrons. According to Table I and Fig. 1 we expect that, compared to free electron impact, the $e-e$ processes, i.e., ionization by bound electrons, should scale in the following manner: 1 for H and He^+ impact, 2 for He impact, 3 for Li impact, 4 for C impact, 6 for O impact, and 8 for Ne impact. Thus, the mea-

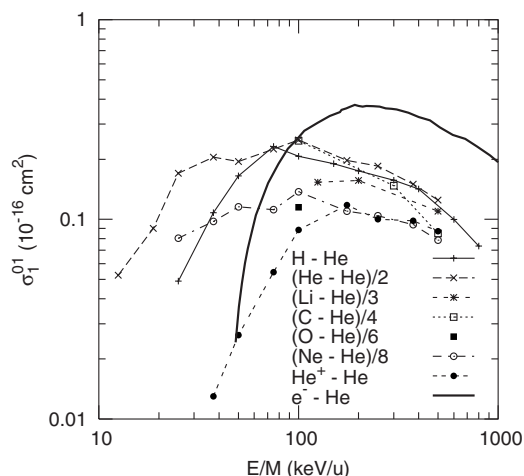


FIG. 3. Comparison of ionization of He by free electrons and by electrons bound on neutral projectiles. Ion and atom data as in Fig. 1, and electron data from Ref. [34].

sured cross sections divided by the expected scaling behavior are shown in Fig. 3. We note that all the bound-electron impact data tend to merge together for impact energies well above threshold but all are considerably smaller than for free electron impact. This may reflect the influence of self-screening by the other projectile electrons which has the effect of reducing N , i.e., the cross sections should be scaled by N_{eff} rather than by N . Also observe the sharper threshold for free electron impact in comparison to those for bound electron impact. This indicates the influence of the projectile momentum distributions associated with $e-e$ processes, and also the influence of second-order $e-n$ effects, which contribute quite strongly for impact energies far below threshold.

V. CONCLUSIONS

An extensive investigation of ionization occurring in atom-atom collisions has been presented. Experimental data covering a rather broad range of neutral projectiles and impact energies have been used to probe the relative importance and scaling behavior of $e-e$ and $e-n$ ionization mechanisms. In addition, ionization of helium by free electrons and ionization by bound electron impact have been compared. From these data and comparisons, it has been shown that neutral atoms tend to induce ionization nearly as efficiently as do singly charged ions even though no long-range Coulomb forces are present. We have also shown that within experimental uncertainties $e-e$ ionization cross sections scale with the number of available projectile electrons, as expected. Finally, we have directly compared the probabilities for ionization of a target atom by free and bound electrons and have found that bound-electron-induced cross sections are systematically smaller than those for free electron impact.

ACKNOWLEDGMENTS

This research was sponsored by U.S. Department of Energy, Office of Basic Energy Sciences, Division of Chemical Sciences under a contract with Martin Marietta Energy Systems, Inc. J.M.S., E.F.D., and J.L.S. acknowledge additional support from ORNL and the Oak Ridge Institute for Science and Education. During preparation of this manuscript, R.D.D. was supported by U.S. DOE, Office of Fusion Energy Sciences, and S.T.M. by U.S. DOE, Office of Basic Energy Sciences, Division of Chemical Sciences.

- [1] R. D. DuBois and A. Kövèr, *Phys. Rev. A* **40**, 3605 (1989).
- [2] E. Horsdal Pedersen and L. Larsen, *J. Phys. B* **12**, 4099 (1979).
- [3] R. D. DuBois and L. H. Toburen, *Phys. Rev. A* **38**, 3960 (1988).
- [4] R. D. DuBois and S. T. Manson, *Nucl. Instrum. Methods Phys. Res. B* **86**, 161 (1994).
- [5] D. R. Bates and G. W. Griffing, *Proc. R. Soc. (London), Ser. A* **68**, 90 (1955).
- [6] K. L. Bell and A. E. Kingston, *J. Phys. B* **2**, 653 (1969).
- [7] K. L. Bell, V. Dose, and A. E. Kingston, *J. Phys. B* **2**, 831 (1969).
- [8] J. S. Briggs and K. Taulbjerg, in *Structure and Collisions of Ions and Atoms*, edited by I. A. Sellin (Springer-Verlag, Berlin, 1976), pp. 105–153.
- [9] R. D. DuBois and S. T. Manson, *Phys. Rev. A* **42**, 1222 (1990).
- [10] S. T. Manson and R. D. DuBois, *Phys. Rev. A* **46**, R6773 (1992).
- [11] E. C. Montenegro, W. S. Melo, W. E. Meyerhof, and A. G. de Pinho, *Phys. Rev. A* **48**, 4259 (1993).
- [12] W. Wu *et al.*, *Phys. Rev. Lett.* **72**, 3170 (1994).
- [13] R. Dörner *et al.*, *Phys. Rev. Lett.* **72**, 3166 (1994).
- [14] W. Wu *et al.*, *Phys. Rev. A* **55**, 2771 (1997).
- [15] H. Kollmus, R. Moshhammer, R. E. Olson, S. Hagmann, M. Schulz, and J. Ullrich, *Phys. Rev. Lett.* **88**, 103202 (2002).
- [16] R. D. DuBois, *Phys. Rev. A* **33**, 1595 (1986).
- [17] R. D. DuBois, *Phys. Rev. A* **36**, 2585 (1987).
- [18] R. D. DuBois, *Phys. Rev. A* **39**, 4440 (1989).
- [19] E. Horsdal Pedersen, J. Heinemeier, L. Larsen, and J. V. Mikkelsen, *J. Phys. B* **13**, 1167 (1980).
- [20] T. R. Dillingham, J. R. Macdonald, and P. Richard, *Phys. Rev. A* **24**, 1237 (1981).
- [21] R. K. Janev, R. A. Phaneuf, and H. T. Hunter, *At. Data Nucl. Data Tables* **40**, 249 (1988).
- [22] J. L. Shinpaugh, Ph.D. thesis, Kansas State University, 1990.
- [23] J. L. Shinpaugh, J. M. Sanders, J. M. Hall, D. H. Lee, H. Schmidt-Böcking, T. N. Tipping, T. J. M. Zouros, and P. Richard, *Phys. Rev. A* **45**, 2922 (1992).
- [24] H. Knudsen, L. H. Andersen, P. Hvelplund, G. Astner, H. Cedergren, H. Danared, L. Liljeby, and K.-G. Rensfelt, *J. Phys. B* **17**, 3545 (1984).
- [25] M. B. Shah and H. B. Gilbody, *J. Phys. B* **18**, 899 (1985).
- [26] Y. Nakai and M. Sataka, *J. Phys. B* **24**, L89 (1991).

- [27] P. Hvelplund and E. Horsdal Pedersen, *Phys. Rev. A* **9**, 2434 (1974).
- [28] K. D. Sevier, *At. Data Nucl. Data Tables* **24**, 323 (1979).
- [29] W. E. Wilson and L. H. Toburen, *Phys. Rev. A* **11**, 1303 (1975).
- [30] D. J. Lynch, L. H. Toburen, and W. E. Wilson, *J. Chem. Phys.* **64**, 2616 (1976).
- [31] L. H. Toburen and W. E. Wilson, *J. Chem. Phys.* **66**, 5202 (1977).
- [32] L. H. Toburen, W. E. Wilson, and L. E. Porter, *J. Chem. Phys.* **67**, 4212 (1999).
- [33] M. E. Rudd, R. D. DuBois, L. H. Toburen, C. A. Ratcliffe, and T. V. Goffe, *Phys. Rev. A* **28**, 3244 (1983).
- [34] M. B. Shah, D. S. Elliott, P. McCallion, and H. B. Gilbody, *J. Phys. B* **21**, 2751 (1988).